# Genetic Recombination in Bacteriophage T4: Single-Burst Analysis of Cosegregants and Evidence in Favor of a Splice/Patch Coupling Model

**Victor P. Shcherbakov, L. A. Plugina and M. A. Nesheva**

*Institute of Chemical Physics in Chernogolovka, Russian Academy of Sciences, Chernogolovka 142432, Moscow Region, Russia*

Manuscript received October 22, 1991
Accepted for publication April 23, 1992

ABSTRACT

To reveal the structure of penultimate DNA intermediates in T4 bacteriophage recombination, resolution of which produces free recombinant molecules, a single-burst analysis of the recombinant progeny was made in multifactor crosses, enabling one to determine quantitatively the different recombinants generated by one or two exchanges within the same chromosome segment. It was found that double and single exchanges are highly correlated in T4 recombination. These results were interpreted as evidence for simultaneous formation of a splice/patch pair as the primary recombination products. A recombination model called here the "splice/patch coupling model" is presented according to which resolution of a single DNA intermediate results in two linear heterozygous molecules containing a patch and a splice, respectively, in homologous positions.

THE numerous observations indicating coupling of general recombination and DNA replication in the life cycle of bacteriophage T4 (*cf.* BROKER and DOERMANN 1975; MOSIG *et al.* 1979) find a substantial explanation in a join-copy recombination model (MOSIG *et al.* 1981; LUDER and MOSIG 1982; MOSIG 1983; DANNENBERG and MOSIG 1983; MOSIG, SHAW and GARCIA 1984), according to which DNA replication is a prerequisite for initiation of recombination, while recombination intermediates serve in turn as the primers for initiation of DNA replication. An extraordinary flexibility of the model, in particular the possibility of multiple pathways for resolution of complex DNA intermediates, endows it with the ability to explain many of the known features of DNA metabolism and the phenotypic properties of various T4 mutants, as well as the remarkable absence of phage mutants with fully blocked recombination.

However, this high flexibility of the join-copy model has its own shortcoming, reducing its heuristic value. The general notion of a DNA recombination intermediate as a primer for initiation of replication (STAHL 1979) when combined with the other elementary recombination processes, such as single- and double-strand exchange, action of endo- and exonucleases and so on, begets a virtually inexhaustible variety of possible recombination pathways, and the problem is to separate actual mechanisms from all the conceivable ones. The common way to resolve such problems is to check specific predictions of the model. A very careful exploration of alternative pathways has enabled us to, indeed, find testable predictions which help to further define the major processes involved.

Figure 1 demonstrates genetic consequences of some of the possible recombination pathways. The majority of the molecular DNA transformations used in the scheme are quite common in model constructions (STAHL 1979; MOSIG 1983; MOSIG, SHAW and GARCIA 1984). The most popular way to start recombination is to invade a double-stranded DNA molecule with a homologous single-stranded terminus, the event designated as strand exchange in this figure. The reaction is presumably catalyzed by *recA*-like proteins such as the *uvsX* gene product (YONESAKI and MINOGAWA 1985; YONESAKI *et al.* 1985; GRIFFITH and FORMOSA 1985; FORMOSA and ALBERTS 1986a,b; HINTON and NOSSAL 1986; HARRIS and GRIFFITH 1987), in cooperation with other proteins such as gp32 and gp-*uvsY* (SHIBATA *et al.* 1980; YONESAKI and MINOGAWA 1989).

The resulting DNA complex **3** with its displaced single-stranded loop (ssD-junction) plays a key role in the majority of modern recombination models beginning with the model of MESELSON and RADDING (1975). It may be further processed in different ways. The D-loop in structure **3** may be cut and hydrolyzed, with the single-stranded terminus being ligated to the 5′-end of the resulting gap (event $\alpha$). Initiation of replication in the Y-junction thus formed (event $\beta$) will release one molecule with parental genotype (**9**) and one (**10**) with single exchanges in equivalent positions of both strands.

Structurally, the ssD-junction is similar to a replication fork. If a single-stranded terminus is used as a primer for initiation of DNA synthesis (not shown) the complex eventually will be resolved into three linear DNA molecules, one of which is recombinant and similar to molecule **10**. However, these two pathways do not appear to be major mechanisms of normal recombination, which has been shown (DOERMANN

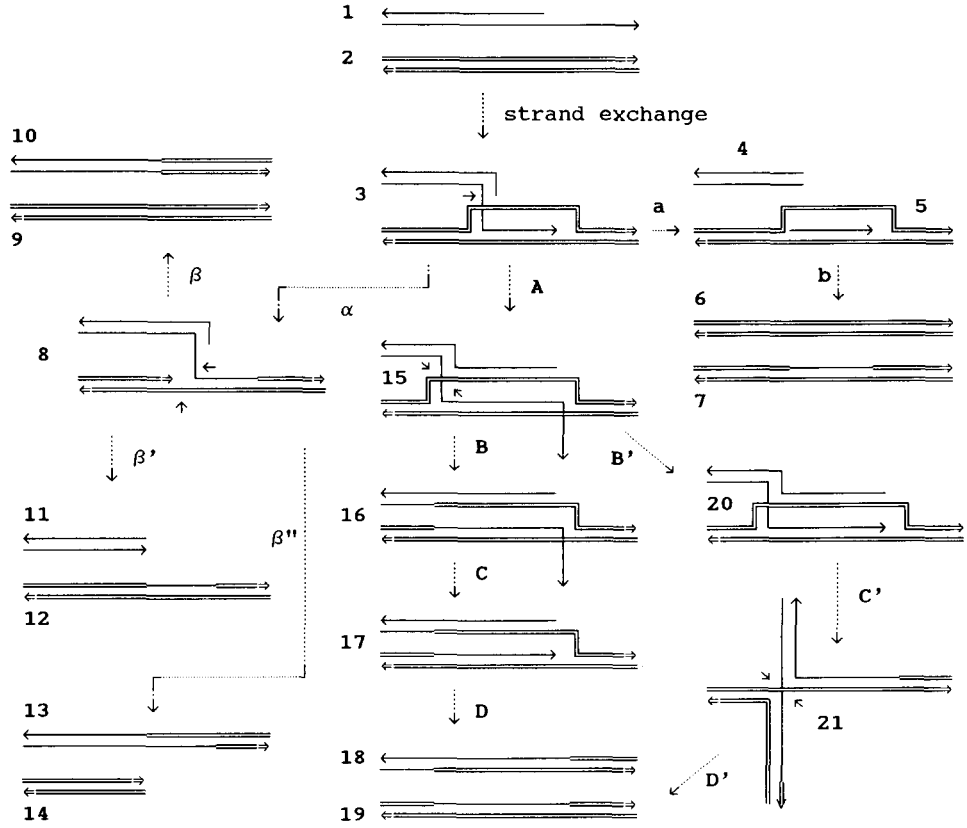


FIGURE 1.—Models for T4 phage recombination. DNA structures and elementary recombination processes are designated by numbers and letters, respectively. DNA strands of different parents depicted with single and double lines, respectively; newly synthesized and parental DNA strands are not distinguished to present more vividly genetic information aspects of the DNA transformations. Arrows at the tips of DNA strands mark 3'OH ends. Small arrows point to the sites of endonuclease action. The parental DNA molecules **1** (with a single-stranded end) and **2** interact via single-strand exchange to produce structure **3** with a displaced loop (ssD-junction). Three ways of further processing the ssD-junction are designated with greek, capital latin and small latin letters, respectively, as follows: ($\alpha$): cutting and hydrolysis of the D-loop followed by ligation of the invading 3'-terminus to the 5'-terminus of the resulting gap; ($\beta$): rightward replication of Y-junction **8**; ($\beta'$) and ($\beta''$): removal of the upper or lower branches of Y-junction **8** leading to formation of a patch (**12**) or a splice (**13**), respectively; A: double-strand exchange; the single-stranded 3'-terminus may become displaced from the complex to form a "whisker"; B: cutting of the cross connection followed by repair of the breaks in dsD-junction **15** leading to formation of Y-junction **16**; C: removal of the whisker by the 3' → 5'-exonuclease of T4 DNA polymerase followed by initiation of replication (event D) leading to heterozygous recombinant molecules **18** and **19** with a splice and a patch, respectively; B': removal of the whisker by the 3' → 5'-exonuclease of T4 DNA polymerase followed by initiation of replication (event C') leading eventually to the Holliday junction **21**; D': endonucleolytic resolution of the Holliday junction; **a**: removal of upper branch of the ssD-junction; **b**: bidirectional replication of molecule **5** resulting in the patch-containing heterozygous molecule **7**.

and BOEHNER 1963; WOMACK 1963; BERGER 1965; WIEMANN 1965; DOERMANN and PARMA 1967; MOSIG 1970) to involve the production of splatches (STAHL 1979): hybrid regions whose flanks are recombinant (splices) or parent (patches). However, one can not exclude that those pathways may operate as a bypass in the absence of some normal functions.

Resolution of the Y-junction **8** by the gene 49 encoded endonuclease VII (JENSCH and KEMPER 1986) gives either a patch (**12**) or a splice (**13**) depending on the cut position, as shown by small arrows (events $\beta'$ or $\beta''$, respectively). Both events produce parental chromosomes *11* or *14* devoid of their termini. In fact, the pathway

$$\alpha \begin{matrix} \rightarrow \beta' \\ \rightarrow \beta'' \end{matrix}$$

represents the well known break-join model (BROKER 1973; BROKER and DOERMANN 1975) according to which each recombination event begets one recombinant molecule and one nonrecombinant stump.

Endonucleolytic cutting of the ssD-junction **3** may also produce splice- or patch-containing DNA intermediates (see structure **5**), on which DNA replication is then initiated (LUDER and MOSIG 1982; MOSIG 1983). Again, the recombination is intrinsically nonreciprocal and only one recombinant product results from a single recombination event (see the event sequence **a** → **b** resulting in patch-containing structure **7** and two parental chromosomes *4* and *6*).

Transition from the single strand- to double strand-exchange in the structure **3** (event **A**) generates a four-stranded complex **15**, in which the D-loop becomes double-stranded (dsD-junction). Perhaps, the

size of the D-loop may be limited because of torsion produced by its propagation, and further migration will displace the single-stranded tip in the form of a "whisker."

Structure **15** has a typical Holliday junction or a cross connection which may be resolved by endonuclease VII (MIZUUCHI *et al.* 1982; KEMPER *et al.* 1984; MUELLER *et al.* 1988), as is shown by small arrows (event **B**). The resulting Y-junction in turn may be either cut by endonuclease VII into linear molecules (not shown), or replicated (event **D**).

A single-stranded whisker may facilitate the initiation of DNA synthesis in the Y-junctions as well as in other recombination intermediates. T4 DNA polymerase is endowed with a very active proofreading 3′ → 5′-exonuclease (ENGLUND 1971; MUZYCZKA, POLAND and BESSMAN 1972; BEDINGER and ALBERTS 1983). The enzyme is specific to 3′OH DNA ends, single-stranded termini being preferentially attacked. Deoxyribonucleoside triphosphates inhibit the nuclease activity against complementary paired ends; hence, this activity is virtually absent *in vivo*. An erroneous inclusion of a noncomplementary nucleotide into the nascent DNA strand provokes exonuclease attack, the enzyme resuming replication after removal of the incorrect nucleotide. If the single-stranded whisker in structures **15** or **16** is hydrolyzed by the 3′ → 5′-exonuclease of T4 DNA polymerase (events **B′** or **C**), consequent immediate initiation of DNA synthesis seems to be inevitable. T4 DNA polymerase alone can carry out such initiation *in vitro* (ENGLUND 1971), while a complex of several proteins, supposedly operating *in vivo*, can do it much more efficiently (BEDINGER and ALBERTS 1983). The results of a detailed study of recombinational effects of gene 43 antimutator allele *tsL42* (V. P. SHCHERBAKOV, L. A. PLUGINA and E. A. KUDRYASHOVA, in preparation) were interpreted as evidence for direct involvement of 3′ → 5′-exonuclease of T4 DNA polymerase in the initial step of general recombination. Though not shown, the protruding 3′-ends are also expected in structures **3**, **5** and **8**; they may appear as a result of branch migration thus promoting initiation of replication.

Evidently, the replication initiated in Y-junction **17** will run only in one direction–to the right in Figure 1–and it will resolve this intermediate into two linear molecules containing a splice (**18**) and a patch (**19**), respectively. The left borders of the patch and splice fall at equivalent chromosome points, whereas the right borders of the splatches, generally speaking, may not coincide.

DNA replication may be initiated in dsD-junction **15** (event sequence **B′** → **C′**) before cutting of the crossed strands. The replication running unidirectionally (to the right) gives eventually the Holliday junction. The latter is physically the same as that postulated by Holliday but the splatches in it are oriented in such a way that cutting of the crossed strands (event **D′**) releases two linear recombinant molecules identical to those resulting from event **D**, *i.e.*, a splice/patch pair arises from the break-down of a single DNA intermediate.

Thus, in the pathway

$$\mathbf{A} \begin{matrix} \rightarrow \mathbf{B'} \rightarrow \mathbf{C'} \rightarrow \mathbf{D'} \\ \rightarrow \mathbf{B} \rightarrow \mathbf{C} \rightarrow \mathbf{D} \end{matrix}$$

the patch and splice arise simultaneously as a consequence of resolution of single DNA intermediate **15**. This prediction seems to be a feature of the models postulating recombination-replication coupling. According to the break-join models, the patches and splices have to arise in independent recombination acts, producing either single recombinant molecules (*e.g.*, pathway

$$\alpha \begin{matrix} \rightarrow \beta' \\ \rightarrow \beta'' \end{matrix}$$

in Figure 1), or the coupled reciprocal pairs patch/patch or splice/splice, as in Holliday's original model (HOLLIDAY 1964). This co-arising of the splice/patch pairs provides an alternative to isomerization of the Holliday structure (SIGAL and ALBERTS 1972; MESELSON and RADDING 1975), which would have to proceed rather quickly to account for the approximately equivalent formation of patches and splices (HURST, FOGEL and MORTIMER 1972; BERGER 1965; TOOMPUU and SHCHERBAKOV 1980). In the DISCUSSION we present some other theoretically conceivable pathways leading (in the recombinational sense) to the same final result.

In conclusion, certain of the possible recombination pathways lead to the coupled formation of two different recombinant products, containing a single and a double exchange, respectively, in homologous positions. To estimate the contribution of these pathways, we have used analysis of T4 recombinants in single bursts from the four-factor crosses in which three different recombinants could be determined separately. The results obtained confirm the predicted splice/patch coupling (SPC) model and show that this pathway does, indeed, play a major role in recombination.

## MATERIALS AND METHODS

**Bacteriophages:** *rIIA* and *rIIB* mutants used in this work are shown in Figure 2. *FC21* and *FC47* are mutations with an opposite phase shift (minus and plus, respectively); they mutually suppress each other, so that the double mutant *FC21-FC47* has rII$^+$ phenotype: it produces wild-type plaques on *Escherichia coli B* and grows efficiently on λ-lysogenic hosts. The origin of the T4 strains was described earlier (SHCHERBAKOV *et al.* 1982a; SHCHERBAKOV and PLUGINA 1991).

**Bacteria:** *E. coli BB* was used to prepare phage stocks and to determine the total titer in lysates from crosses; *E. coli B*

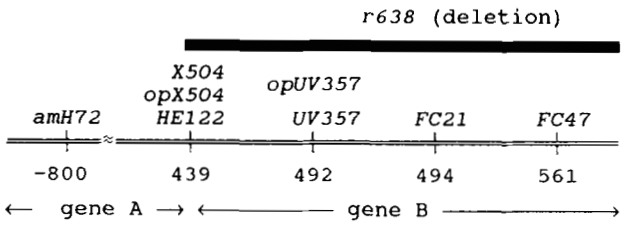


FIGURE 2.—Map positions of the *rII* mutants used in the study. Numbers under the mutant sites designate their coordinate on the *rII* sequence (PRIBNOW *et al.* 1981). The position of *amH72* has been determined approximately by recombination data. The mark ≈ is used to stress that the interval *amH72-HE122* is much longer than the others. The mutations *amH72* and *HE122* are *amber* (UAG) suppressible; ocher (UAA) mutations *X504* and *UV357* behave as non-suppressible on the *E. coli*(λ) strains we used; *opX504* and *opUV357* are opal (UGA) suppressible; *FC21* and *FC47* are minus and plus frameshift mutations, respectively, suppressing each other, the double *FC21-FC47* having fully *rII*$^+$ phenotype.

served as a host in phage crosses and as the indicator strain to discern r$^+$ and r phenotypes. *E. coli K223* is a λ-lysogenic strain carrying a UGA-suppressor. It is permissive for opal *rII* mutants and is not permissive for other *rII* mutants. *E. coli CA180* and *CA265* are λ-lysogenic UAG-suppressor strains permissive for amber mutants. *E. coli 594*(λ), restrictive for all *rII* mutants, was used to determine the titer of recombinants with *rII*$^+$ phenotype.

**Media, management of bacterial cultures and the procedure for standard crosses:** These were as described earlier (SHCHERBAKOV *et al.* 1982a).

**Single burst experiment:** Our approach was based on methodology analogous to that developed by ELLIS and DELBRUCK (1939). *E. coli B* was grown aerobically at 33° in L-broth to a cell concentration of $2 \cdot 10^8$ per ml. To 0.5 ml of the bacterial suspension 0.1 ml of 0.02 M sodium cyanide was added, the suspension was held for 1 min at room temperature, and then a mixture of phage parents in a volume of 0.5 ml was added to provide a nominal multiplicity of infection for each recombining parent of one phage particle per bacterium. The recombinationally inert deletion marker *r638* (diluent) was included in the cross to diminish the rate of recombination in the region under examination (the total multiplicity of infection was adjusted to ten per bacterium). The more rapidly lysed *E. coli B* instead of our usual host *E. coli BB* was also used for the same purpose. The infected cells were incubated for 10 min at 33° and then diluted with ice-cold L-broth to a concentration that corresponded to an average of one recombinant phage particle per ml. The diluted cold culture was pipetted into 300 test tubes, 0.1 ml each, so that about 90% of the tubes contained no recombinant particles. The tubes were incubated in a moist box at 36° for 2 hr. Then, 0.5 ml of L-broth saturated with chloroform was added to each tube to complete lysis. Melted soft agar (2.5 ml) was added, and the entire contents of the tube was plated either on *E. coli CA180*, on which *rII*$^+$ and *amber* recombinants produce plaques, or on *E. coli K223*, on which *rII*$^+$ and *opal* recombinants grow, the parents being unable to grow on either strain. The plates were incubated overnight, and all the plaques formed were picked up and spot-tested on *E. coli 594*(λ) to distinguish *rII*$^+$ recombinants from those of *amber* or *opal* type.

Multiple yields from the lawns of *E. coli CA180* (*i.e.*, when two or more recombinant particles were found in a tube) were also plated on *E. coli B* to check for secondary recombinants. The crosses under study are not expected to generate nonrecombinant heterozygous particles able to form

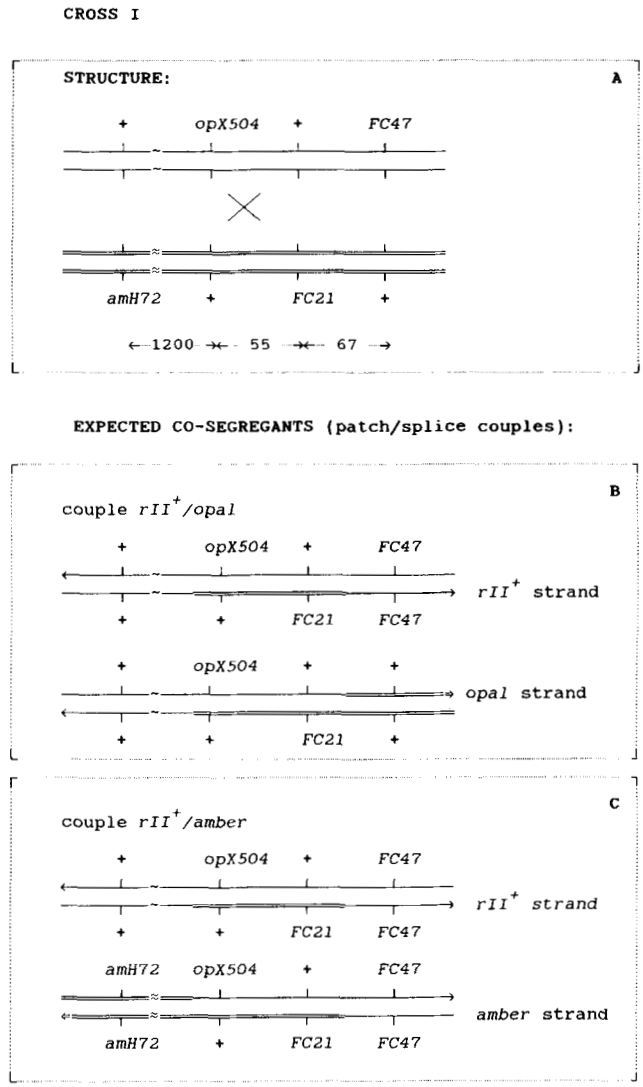


FIGURE 3.—Structure of the four-factor cross I and primary recombinant products predicted by the SPC model. A: Structure of the cross; numbers show the lengths of the genetic intervals in bp. B: Recombinant couple expected to be recovered after plating on opal-suppressor host *E. coli K223*. C: Recombinant couple expected to be recovered after plating on amber-suppressor host *E. coli CA180*. Marks ~ or ≈ are used to stress that the interval *amH72-opX504* is much longer than the others.

plaques on lawns of the λ-lysogenic indicator *E. coli* strains. For example, terminal heterozygote in cross I *amH72-FC21/opX504-FC47* cannot multiply on *E. coli CA180* because of the absence of the functional *rIIB*$^+$ gene. However, during growth of the plaques originating from recombinant particles, secondary recombinants can arise in some special cases, thus affecting the results of the consequent spot-test on *594*(λ). Indeed, owing to terminal redundancy, recombinant chromosomes *amH72-FC21-FC47* (of amber phenotype) in cross I (Figure 3) have a certain probability of getting two sets of *rII* genes, terminal heterozygotes of the type *amH72-FC21-FC47/opX504-FC47*. *CA180* cells infected with such heterozygotes have a rather high probability of producing the recombinant *FC21-FC47* (rII$^+$) during the first round of phage multiplication. The resulting plaque would contain a mixture of *amber* and *rII*$^+$ progeny particles giving a false-positive spot on *594*(λ). The probability that such recombinant heterozygotes arise seems to be low: the frequency of terminal redundancy heterozygotes is about 0.5–0.7% (Mo-

SIG 1970). Though preferential initiation of DNA packaging at the recombinational branch points (MOSIG, GHOSAL and BOCK 1981) can enhance the frequency of terminal heterozygotes among recombinant progeny 3-fold (V. P. SHCHERBAKOV, L. A. PLUGINA and M. A. NESHEVA, in preparation), the expected contribution of the secondary recombinants remains too low to affect significantly the appearance of mixed recombinant yields.

Nevertheless, we checked all the plaques in multiple yields from *E. coli CA180* for secondary recombination. From the total 474 recombinant plaques analyzed in cross I, 10 (2.2%) were found to contain mixed progeny, and in only one case of 13 did this information influence the final proportion of tubes with mixed yields.

In the case of recombinants picked up from the *K223* lawns in the same cross, the terminal heterozygote interference is expected to be negligible, because only a double exchange in a rather short interval could produce wild-type recombinants from the corresponding heterozygotes, so we did not analyze those recombinants for secondary recombination.

## RESULTS

**Preliminary methodological considerations:** To determine the extent of possible coupling of splice and patch formation in the course of recombination, we analyzed the recombinants from single bursts in the crosses shown in Figure 3 (cross I) and in Figure 4 (cross II).

In cross I, recombinant *FC21-FC47*, which is phenotypically rII$^+$, can arise from a single recombination event provided two sites–*opX504* and *FC21*–fall in the same patch. The interval *opX504-FC21* is small enough, when compared to the mean patch length, that the probability for such an event is nearly as high as that for a one point marker to be captured by the patch. Different ways to estimate hDNA length in T4 gave similar values, about 400 bp (BERGER 1965; WIEMANN 1965; BROKER 1973; TOOMPUU and SHCHERBAKOV 1980; V. P. SHCHERBAKOV, L. A. PLUGINA and E. A. KUDRYASHOVA, in preparation). According to the SPC model, recombinants *opX504* (*opal*) and *amH72-FC21-FC47* (*amber*) can arise in various recombination events, while their simultaneous formation with the pseudowild *FC21-FC47* is possible only if the patch and the splice occupy the relative positions shown in Figure 3, B and C, respectively.

To provide productive infection in a λ-lysogenic cell, the *rII* function must be expressed before DNA replication (EDGAR 1961; GAREN 1961). This means that only half of the primary recombinant heterozygotes produce plaques on indicator strains selecting for the recombinants, namely those with the functional sense DNA strand. In Figure 3B, the chromosome strand with the double exchange has the same polarity as the recombinant strand in the chromosome with the single exchange; hence, the correlated formation of the patch and the splice may be revealed whether or not the heterozygous chromosomes were replicated before encapsidation. In contrast, as is seen from Figure 3C, the recombinant strands of pseudowild and *amber* type have opposite orientations, their co-arising being observable only if at least one of the two primary heterozygous DNA molecules was replicated (or corrected) before encapsidation.

The *amH72-FC21-FC47* genotype of the *amber*-type recombinants and *FC21-FC47* genotype of *rII*$^+$ recombinants in the cross *H72-FC21* × *opX504-FC47* was directly checked as follows. Five plaques originating from the *CA180* lawn and having amber phenotype [negative spot-test on *594*(λ)] were cloned and crossed against *rIIB* mutant *FC21*. The lysates were plated on *594*(λ). Five recombinant plaques (supposedly, *FC21-FC47*) from each cross were picked up, cloned, crossed against true wild-type phage and the lysates were plated on *E. coli B*, on which expected *rII* recombinants could be distinguished from the parents that both have wild-type phenotype. Five r-plaques from each lysate were picked up, cloned and backcrossed against *FC21* and *FC47*. All the plaques were identified as either *FC21* or *FC47*. These results prove the *amH72-FC21-FC47* genetic structure of the amber recombinants in cross I. Similarly, the genotypes of five *rII*$^+$ recombinants [positive spot-test on *594*(λ)] were proved to be *FC21-FC47*. Thus, from 10 recombinants analyzed none was found to be *amH72* or true *rII*$^+$. The latter recombinants are expected to be rare in this cross: *amH72* can be generated by a very short patch covering only site *FC21*, while a triple exchange is needed for creation of true *rII*$^+$ in cross I.

If the recombination pathway with the splice/patch coupling is the only one operating during T4 multiplication, the cases depicted in Figure 3 exhaust all of the possible variants of the events resulting in formation of pseudowild *FC21-FC47*, *i.e.*, the patch covering the interval *opX504-FC21* is always coupled either with the splice as shown in Figure 3B, or with that shown in Figure 3C. In other words, given that the *FC21-FC47* recombinant has arisen, one should expect formation of an *opal* recombinant with a probability of 0.5. As to the correlation of *rII*$^+$/*amber* (Figure 3C), the matter is complicated with two peculiarities. First, simultaneous formation of recombinant strands *FC21-FC47* and *amH72-FC21-FC47* is possible only if the right border of the splice falls in the same short interval, *FC21-FC47*, in which the right border of the patch has fallen. This coincidence may occur with significant frequency only if the patch and the splice do not differ significantly in their lengths. The second complication is related to the opposite polarity of the coincident recombinant strands, as mentioned above. Both of these factors are expected to reduce the value of the *rII*$^+$/*amber* correlation as compared to that of *rII*$^+$/*opal*.

Mismatch repair in heteroduplex intermediates may also somewhat distort the single-burst data. All the markers used in our crosses, except *opX504*, are non-repairable (SHCHERBAKOV and PLUGINA 1991). Repair

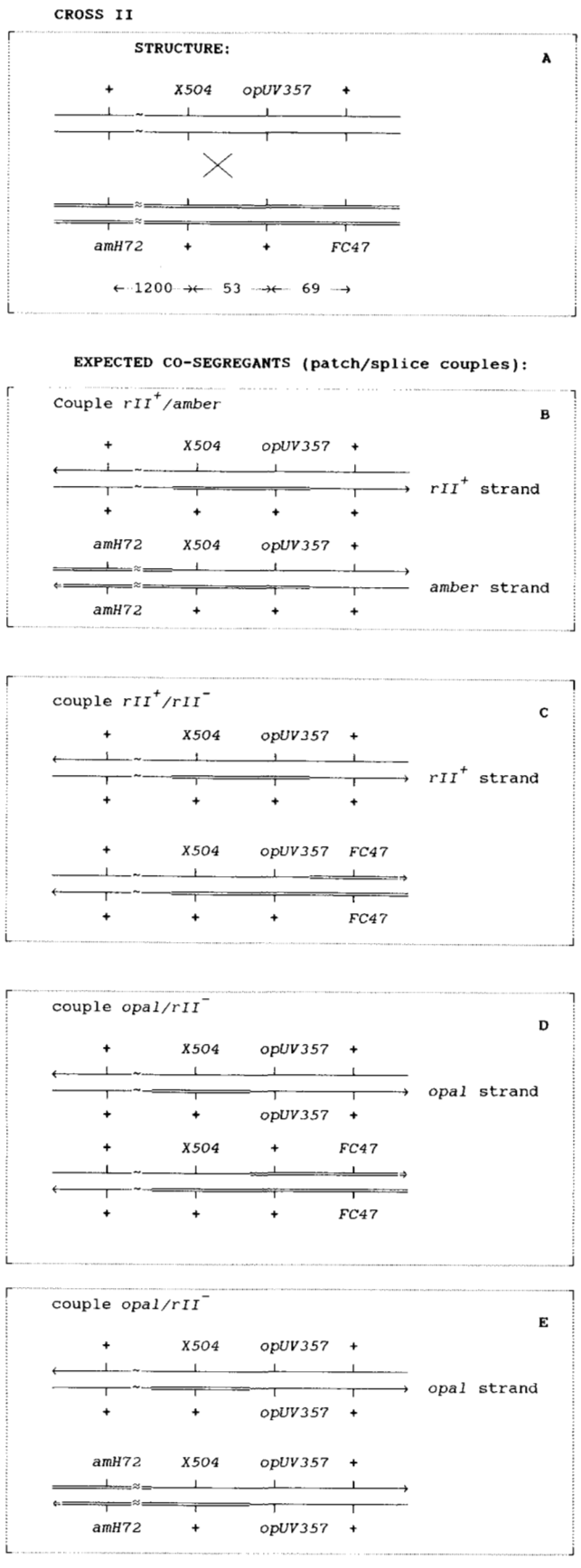


of mismatches *opX504*/+ in heteroduplexes shown in Figure 3B either does not change or diminishes the apparent coupling. For example, correction of the *opal* strand to $rII^+$ strand produces the couple $rII^+/rII^+$, thus eliminating mixed yield. None of the repair events could produce mixed yield. The same is true for the couple of heteroduplexes shown in Figure 3C. It is evident that multiple recombinant yields due to replication can not be changed by repair.

If recombination goes via independent formation of patches and splices or if hybrid regions are not formed at all, as is shown at the left side of the Figure 1, then one should not expect any correlation between the appearance of different recombinants.

In principle, the correlated formation of different recombinants can be observed by analyzing recombinant progeny from single bursts. However, a number of practical obstacles and quantitative limitations should be considered. The mixed recombinant yields, *e.g.*, $rII^+$ + *opal*, may result not only from their coupled formation, but also from the coincidence of two independent events either in the same cell or in two different cells in the same test tube.

The interference of the latter type can be reduced to any acceptable value by increasing the extent of dilution of the infected culture (unfortunately, with an inevitable increase in the laboriousness) and its value can be easily calculated in accordance with the Poisson distribution. The interference of the former type (in-the-same-cell coincidence) can be reduced only by reducing the rate of intracellular recombination. To achieve this, we used very closely linked markers and introduced in the crosses the recombinationally inert deletion *rII* mutant *r638* as diluent.

In preliminary experiments, we analyzed the distribution of total yields among individual *E. coli B* cells. The maximum yields never exceeded 500 (median = 200) phage particles per cell. The frequencies of recombinants growing on *E. coli 594*(λ), *K223* and *CA180*, as determined in a standard cross *amH72-FC21* × *opX504-FC47* × *r638* at multiplicities of infection of 1, 1 and 8, respectively, were found to be equal to $3.4 \cdot 10^{-5}$, $1.5 \cdot 10^{-4}$ and $1.5 \cdot 10^{-4}$, respectively (Tables 1 and 2). A similar range of recombinant frequencies was observed in crosses II and III (Tables 3–5).

At this level of recombinant frequencies and phage yields there remains some significant contribution of

FIGURE 4.—Structure of the four-factor cross II and primary recombinant products predicted by the SPC model. A: Structure of the cross; numbers show the lengths of the genetic intervals in bp. B: Recombinant couple $rII^+/amber$ expected to be recovered after plating on amber-suppressor host *E. coli CA180*. C: Recombinant couple $rII^+/rII^-$; only $rII^+$ can produce plaques on *CA180*. D and E show recombinant pairs co-arising when site *X504* falls in a patch; only the opal recombinant produces plaques on *K223* host. Marks ~ or ≈ are used to stress that the interval *amH72-X504* is much longer than the others.

TABLE 1

**Analysis of *rII*$^+$ and *opal* recombinants in single burst experiments: cross I, *amH72-FC21* × *opX504-FC47* (Figure 3)**

| Item | Quantitative characteristics |
|---|---|
| No. of independent experiments | 6 |
| Frequencies of recombinants in standard crosses: | |
| *rII*$^+$ (growth on *594*(λ)) | $3.23 \cdot 10^{-5}$ |
| *rII*$^+$ + *opal* (growth on *K223*) | $1.50 \cdot 10^{-4}$ |
| Total no. of test tubes analyzed | 1800 |
| No. of tubes with one recombinant particle | 105 |
| No. of tubes with more than one recombinant particle | 44 |
| No. of tubes with *rII*$^+$ recombinants only | 35 |
| No. of tubes with *opal* recombinants only | 97 |
| No. of tubes with a mixture of *rII*$^+$ + *opal* recombinants | 17 |
| Expected no. of mixed yields resulting from random coincidence of independent events | 3[a] |
| Proportion of "true" mixed yields in the total no. of the yields containing *rII*$^+$ recombinants | 0.29 ± 0.04[b] |

[a] The value was calculated separately for each of six experiments and then summed.

[b] The mean with respect to six independent determinations and standard deviation of the mean is given. The calculations based on the summed data, as presented in the Tables 1–5, may give somewhat different proportion values, but such calculations are not strictly correct.

TABLE 2

**Analysis of *rII*$^+$ and *amber* recombinants in single burst experiments: cross I, *amH72-FC21* × *opX504-FC47* (Figure 3)**

| Item | Quantitative characteristics |
|---|---|
| No. of independent experiments | 13 |
| Frequencies of recombinants in standard crosses: | |
| *rII*$^+$ (growth on *594*(λ)) | $3.44 \cdot 10^{-5}$ |
| *rII*$^+$ + *amber* (growth on *CA180*) | $1.50 \cdot 10^{-4}$ |
| Total no. of test tubes analyzed | 3900 |
| No. of tubes with one recombinant particle | 202 |
| No. of tubes with more than one recombinant particle | 140 |
| No. of tubes with *rII*$^+$ recombinants only | 100 |
| No. of tubes with *amber* recombinants only | 198 |
| No. of tubes with a mixture of *rII*$^+$ + *amber* recombinants | 44 |
| Expected no. of mixed yields resulting from random coincidence of independent events | 9[a] |
| Proportion of "true" mixed yields in the total no. of yields containing *rII*$^+$ recombinants | 0.24 ± 0.03[b] |

[a] The value was calculated separately for each of 13 experiments and then summed.

[b] The mean with respect to 13 independent determinations and standard deviation of the mean is given.

in-the-same-cell coincidence to apparent recombinant coupling. For example, in the cross *amH72-FC21* × *opX504-FC47* × *r638* the probability of appearance of an *rII*$^+$ recombinant in one cell (assuming yield = 200)

TABLE 3

**Analysis of *rII*$^+$ and *amber* recombinants in single burst experiments: cross II, *amH72-FC47* × *X504-opUV357* (Figure 4)**

| Item | Quantitative characteristics |
|---|---|
| No. of independent experiments | 6 |
| Frequencies of recombinants in standard crosses: | |
| *rII*$^+$ (growth on *594*(λ)) | $4.98 \cdot 10^{-5}$ |
| *rII*$^+$ + *amber* (growth on *CA180*) | $8.33 \cdot 10^{-5}$ |
| Total no. of test tubes analyzed | 1800 |
| No. of tubes with one recombinant particle | 217 |
| No. of tubes with more than one recombinant particle | 95 |
| No. of tubes with *rII*$^+$ recombinants only | 81 |
| No. of tubes with *amber* recombinants only | 190 |
| No. of tubes with a mixture of *rII*$^+$ + *amber* recombinants | 41 |
| Expected no. of mixed yields resulting from random coincidence of independent events | 16[a] |
| Proportion of "true" mixed yields in the total no. of the yields containing *rII*$^+$ recombinants | 0.22 ± 0.04[b] |

[a] The value was calculated separately for each of six experiments and then summed.

[b] The mean with respect to six independent determinations and standard deviation of the mean is given.

TABLE 4

**Analysis of *rII*$^+$ and *opal* recombinants in single burst experiments: cross II, *amH72-FC47* × *X504-opUV357* (Figure 4)**

| Item | Quantitative characteristics |
|---|---|
| No. of independent experiments | 6 |
| Frequencies of recombinants in standard crosses: | |
| *rII*$^+$ (growth on *594*(λ)) | $4.98 \cdot 10^{-5}$ |
| *rII*$^+$ + *opal* (growth on *K223*) | $1.77 \cdot 10^{-4}$ |
| Total no. of test tubes analyzed | 1800 |
| No. of tubes with one recombinant particle | 154 |
| No. of tubes with more than one recombinant particle | 52 |
| No. of tubes with *rII*$^+$ recombinants only | 126 |
| No. of tubes with *opal* recombinants only | 63 |
| No. of tubes with a mixture of *rII*$^+$ + *opal* recombinants | 17 |
| Expected no. of mixed yields resulting from random coincidence of independent events | 10[a] |
| Proportion of "true" mixed yields in the total no. of yields containing *rII*$^+$ recombinants | 0.06 ± 0.02[b] |

[a] The value was calculated separately for each of six experiments and then summed.

[b] The mean with respect to six independent determinations and standard deviation of the mean is given.

is expected to be $3.4 \cdot 10^{-5} \cdot 200 = 6.8 \cdot 10^{-3}$. The corresponding probability for the *amber* recombinant would be $1.5 \cdot 10^{-4} \cdot 200 = 3.0 \cdot 10^{-2}$. The latter value is also the probability for any cell containing an *rII*$^+$ recombinant to contain also the (independently arising) recombinant of *amber* type. The calculated value may be somewhat underestimated, since cell-to-cell

**TABLE 5**

**Analysis of *rII*$^+$ and *amber* recombinants in single burst experiments: cross III, *X504* × *UV357* × *HE122-UV357* (Figure 5)**

| Item | Quantitative characteristics |
|---|---|
| No. of independent experiments | 5 |
| Frequencies of recombinants in standard crosses: | |
| *rII*$^+$ (growth on *594*(λ)) | $6.56 \cdot 10^{-5}$ |
| *rII*$^+$ + *amber* (growth on *CA265*) | $1.54 \cdot 10^{-4}$ |
| Total no. of test tubes analyzed | 1500 |
| No. of tubes with one recombinant particle | 145 |
| No. of tubes with more than one recombinant particle | 61 |
| No. of tubes with *rII*$^+$ recombinants only | 97 |
| No. of tubes with *amber* recombinants only | 96 |
| No. of tubes with a mixture of *rII*$^+$ + *amber* recombinants | 13 |
| Expected no. of mixed yields resulting from random coincidence of independent events | 9[a] |
| Proportion of "true" mixed yields in the total no. of yields containing *rII*$^+$ recombinants | 0.032 ± 0.023[b] |

[a] The value was calculated separately for each of five experiments and then summed.

[b] The mean with respect to five independent determinations and standard deviation of the mean is given.

unevenness in yield values will enhance the probability for the coincidence. At maximum yield = 500 we expect 7.5% of all the cells containing an *rII*$^+$ recombinant to contain also an *amber* one. This background is small enough to enable one to observe rather high splice/patch correlation as predicted by the SPC model.

**Cross I:** The structure of the cross and the primary (heterozygous) recombinant products predicted by the SPC model are shown in Figure 3.

*Study of rII*$^+$*/opal correlation*: The results of single-burst experiments in which recombinants with rII$^+$ and opal phenotypes were studied are presented in Table 1. Since recombinant-negative tubes constituted 92% in these experiments, one may infer that in the majority of the positive tubes the recombinants originated from the same cell. Most importantly, 14 tubes with the mixture *rII*$^+$ + *opal* may be considered as containing "cosegregants" (we remember that part of this apparent cosegregation results from the "in-the-same-cell coincidence").

Quantitatively, the data in Table 1 seem to be in agreement with the predictions of the SPC model. According to it, any patch generating rII$^+$ (*FC21-FC47*) obligatorily coincides either with the splice generating *amber* or with the splice generating *opal*. So the mixtures of *rII*$^+$ + *opal* should constitute 50% of all the cases of *rII*$^+$ formation, while we observed 29%. It is evident, however, that a pair of cosegregants may be observed only if both have arisen as DNA molecules and both have been encapsidated. Thus, in practice, we should expect the correlation to be less than 50%. The possible losses are difficult to estimate, but they are expected to be rather large, since the majority of recombinants seem not to undergo extensive replication before packaging. Note that more than half of the positive tubes contain only one recombinant particle. Repair of the mismatch *opX504*/+ may also diminish the apparent coupling.

*Study of rII*$^+$*/amber correlation*: The single-burst experiments in which we analyzed the *rII*$^+$ and *amber* recombinant progeny (Table 2) revealed that recombinant pairs *rII*$^+$*/amber* can also arise from single recombination events. Mixed yields constituted 24% of all the yields containing *rII*$^+$. This value does not differ significantly from the level of *rII*$^+$*/opal* coupling (29%), despite the opposite polarity of the recombinant strands in the primary recombinant progeny, as discussed above. This result means that the probability for at least one of the two heteroduplex cosegregants to be replicated is fairly high. After the first round of replication a heterozygote is converted into a homozygote but remains single, so this statement may not contradict the above remark on the absence of extensive multiplication of the recombinants before packaging limiting the recovery of cosegregants. So we conclude that most of the recombination events leading to formation of *rII*$^+$ recombinants produce simultaneously either *amber* or *opal* recombinants. This is just what was predicted by the SPC model.

**Cross II:** The structure of the cross and the expected recombinant products are shown in Figure 4.

*Study of rII*$^+$*/amber correlation*: Wild-type recombinants in this cross can arise from a single recombination event provided two sites–*X504* and *opUV357*–fall in the same patch. Simultaneous formation of *rII*$^+$ and *amber* recombinant (*amH72*) is possible if the patch and the splice occupy the relative positions shown in Figure 4B. The limitations in coupling recovery in this case are the same as those in cross I for the couple *FC21-FC47/amH72-FC21-FC47* discussed above. They are related to the opposite polarity of the recombinant strands and the limited possibility for the right borders of the patch and splice to fall in the same short interval *opUV357-FC47*.

The results of single-burst experiments in which *rII*$^+$ and *amber* recombinants were studied (Table 3) revealed that recombinant couples *rII*$^+$*/amber* arise from a single recombination event: mixed recombinant yields constituted 22% of all the yields containing *rII*$^+$. The observed correlation was virtually the same as in cross I for the *rII*$^+$*/amber* coupling, in agreement with the SPC model predictions.

*Study of rII*$^+$*/opal correlations*: The recombinants *rII*$^+$ and *opal* are generated in cross II by different patches, covering sites *X504-opUV357* (recombinant *rII*$^+$, Figure 4, B and C) or site *X504* (*opal* recombinant, Figure 4, D and E), respectively. According to the SPC model, these recombinants have to arise in

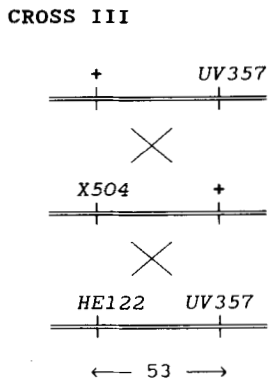


FIGURE 5.—The structure of cross III (three-parental). The size of the interval, in bp, is indicated.

independent events. As is shown in Table 4, mixed (*rII*$^+$ + *opal*) yields constituted 6% of all the yields containing *rII*$^+$. This value is significantly lower than the coupling value (22%) for the couple *rII*$^+$/*amber* in the same cross, and it does not differ significantly from the expected value for in-the-same-cell coincidence.

**Cross III:** The observation made in cross II, namely, high correlation between the double- and single-exchange recombination products and low correlation between the different double-exchange products, might be considered as a strong argument in favor of the reality of the observed correlations. Additional evidence against their artefactual origin was obtained in single-burst experiments using a cross system in which two different recombinants could be formed only in two independent events within the same short chromosomal segment.

In the three-parental system shown in Figure 5, wild-type recombinants arise in the subcross *X504* × *UV357*, whereas recombinants of *amber* type *HE122* can be produced only in the subcross *X504* × *HE122-UV357*. The physical distance between recombining markers (53 bp) was similar to that in crosses I and II. The recombinationally inert fourth parent *r638* was introduced in the cross to diminish the final recombinant frequencies. The multiplicities of infection for the *UV357*, *X504*, *HE122-UV357* and *r638* phages were 1, 1, 1 and 7 particles per bacterium, respectively.

The observed proportion of tubes containing a mixture of recombinants *rII*$^+$ + *amber* (3.2% of all the tubes with *rII*$^+$) may be fully accounted for by the contribution of the in-the-same-cell coincidence (Table 5).

## DISCUSSION

Our direct experimental observation is as follows: in single burst analysis of the four-factor crosses *amH72-FC21* × *opX504-FC47* and *amH72-FC47* × *X504-opUV357* the couples of recombinants *FC21-FC47/opX504* and *FC21-FC47/amH72-FC21-F47* in cross I as well as *rII*$^+$/*amH72* couple in cross II were observed significantly more frequently than would expected if they were formed in independent recombination events. Stringent control measures taken encourage us to conclude with certainty that these recombinant pairs co-arise in single events. Judging from the design of the crosses I and II (Figures 3 and 4), the observed correlations reflect the corresponding linkage between the double and single exchanges.

A release of two recombinant DNA molecules carrying patch and splice, respectively, via processing of one precursor DNA complex seems to be the most easily conceived mechanism for such linkage. The pathway

$$\mathbf{A} \begin{matrix} \rightarrow \mathbf{B}' \rightarrow \mathbf{C}' \rightarrow \mathbf{D}' \\ \rightarrow \mathbf{B} \rightarrow \mathbf{C} \rightarrow \mathbf{D} \end{matrix}$$

shown in Figure 1 yields the necessary splice/patch coupling. The genetic consequences of this coupling in the crosses I and II are demonstrated in Figures 3 and 4 where DNA molecules corresponding to the structures **18** and **19** in Figure 1 carry genetic markers.

According to the SPC model, simultaneous formation of recombinants *FC21-FC47* and *amH72-FC21-FC47* (Figure 3C) is possible only if the right borders of the patch and the splice fall in the same short interval *FC21-FC47*. A similar limitation is also true for the couple *rII*$^+$/*amH72* in cross II (Figure 4B). At a first glance, this limitation is too strong to allow a significant coupling to occur. While the left borders of the splatches in Figures 3C and 4B and the right ones in Figures 3B and 4C occupy homologous sites automatically as a result of breakdown of the crossed strands by endonuclease VII, and while the left ends of the splatches in Figure 3B must nearly always fall in the same large (about 1200 bp) interval *amH72-opX504*, the right ends of the splatches in Figures 3C and 4B may both fall in the interval *FC21-FC47* or *opUV357-FC47* only if the coupled patches and splices have hDNA of nearly equal lengths.

It is probable, however, that the mechanism for the alignment of hDNA borders in splice/patch couples is an intrinsic feature of the double-strand exchange (event **A** in Figure 1). Suppose that the cross connection in structure **3** runs unidirectionally (to the left) until the single-stranded D-loop becomes fully double-stranded. The resulting dsD-junction **15**, being energetically in its most favorable configuration, may not undergo further migration until replication initiation or cutting of the cross connection. In such a case, the patch and splice will always occupy equal and homologous chromosome segments.

The particular version of the SPC model shown in Figure 1 is a variant of the join-copy model rather well substantiated in the above cited papers by G. MOSIG and collaborators. Still, we would like to stress

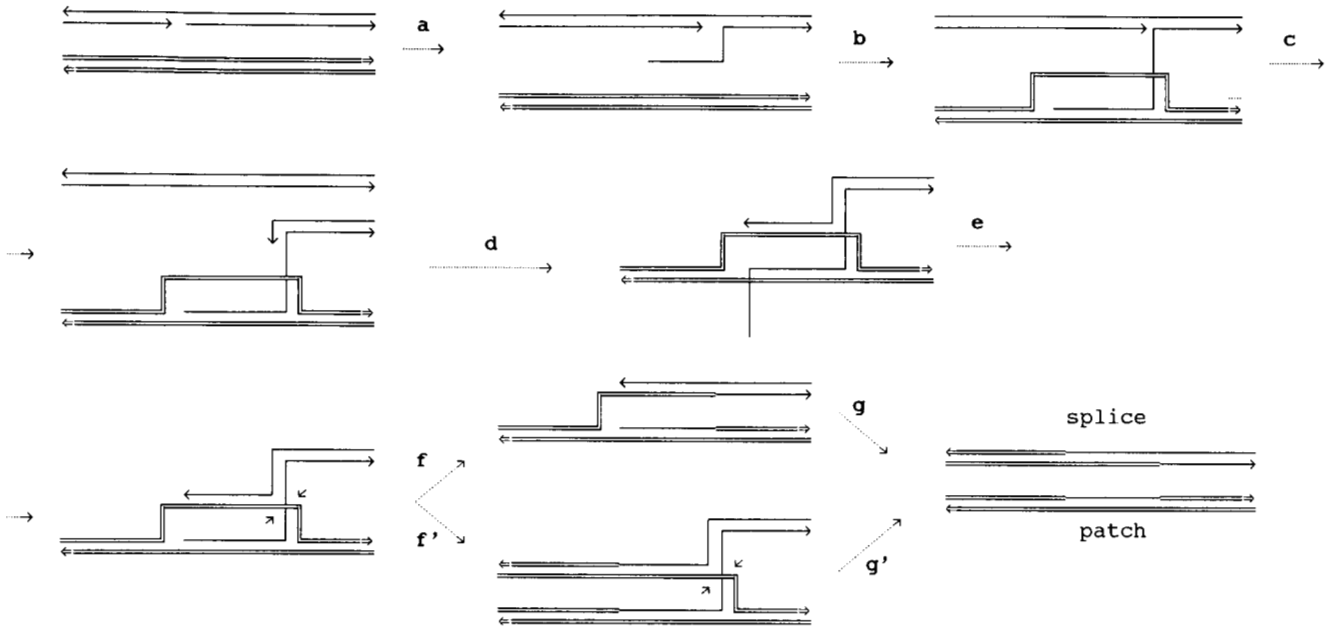


FIGURE 6.—SPC model variant with initiation of recombination via strand-displacement synthesis. DNA strands of different parents are depicted with single and double lines, respectively; newly synthesized and parental DNA strands are not distinguished to present more vividly the genetic information aspects of the DNA transformations. Arrows at the tips of DNA strands mark 3′OH ends. Small arrows points to the sites of endonuclease action. **a**: Strand displacement synthesis originating from a nick results in production of 5′ single-stranded end. **b**: Strand exchange results in production of an ssD-junction. **c**: Rightward replication of the upper chromosome releases one parental DNA molecule from the original ssD-junction. **d**: Double-stranded branch migration accompanied by 5′-end displacement. **e**: Removal of the whisker (by a 5′-exonuclease). **f**: Cutting of the cross connection. **f′**: Leftward replication of the dsd-junction. **g**: Leftward replication of the Y-junction. **g′**: Cutting of the cross connection.

that in its essence the SPC model is not obligatorily tied to chromosomal tips as recombinogenic DNA structures. For example, recombination initiation via strand displacement synthesis from a nick (MESELSON and RADDING 1975; KODADEK and WONG 1990) can also lead to a splice/patch coupling as is shown in Figure 6. In that case, as well as in the scheme shown in Figure 7, the replication/recombination linkage is also postulated, and the correlation observed here may argue in favor of this linkage. We stress that any other model for T4 recombination must be able to explain the coupling of double and single exchanges in homologous regions of the two chromosomes. In particular, models with only one recombinant final product, such as those in the left part of Figure 1, should be ruled out as a major recombination pathway.

Which of the three pathways, as shown in Figures 1, 6 and 7, all giving splice/patch coupling, is preferred? The least probable may be that in Figure 7. The event sequence **a** → **b** → **c** → **d** in this scheme does not include secondary (recombinational) initiation of replication. Quite the contrary, being promoted by replication, it leads to its premature termination. Given that this pathway becomes dominant in some mutant conditions, the DNA will cease its replication prematurely. It is tempting to explain the DNA arrest phenotype of recombinational T4 mutants, such as those in genes 46 and 47 (EPSTEIN *et al.* 1963, SHAH and BERGER 1971), by the prevalence of similar recombination pathways.

As for the recombination initiated with chromosomal tips or with strand displacement DNA synthesis both leading to splice/patch coupling and recombinational initiation of DNA replication, we have no crucial arguments to prefer one of them. On the one hand, the chromosomal tips are recombinogenic (WOMACK 1963; DOERMANN and PARMA 1967; MOSIG 1963; MOSIG *et al.* 1971), evidently because of incomplete replication of the 3′ end of the template for the lagging DNA strand (WATSON 1972). Invasion of this end into double helix provides an elegant way to prime DNA replication. On the other hand, late in infection T4 DNA becomes highly concatemeric (DOERMANN 1973; UHLENHOPP, ZIMM and CUMMINGS 1974; HAMLETT and BERGER 1975; CURTIS and ALBERTS 1976; HAMILTON and PETTIJOHN 1976; KEMPER and JANZ 1976; KOZINSKI and KOSTURKO 1976; SHAH and DELORENZO 1977; MINOGAWA *et al.* 1983) and, hence, with relatively few ends, while the rate of recombination is enhanced during latent period (V. P. SHCHERBAKOV and L. A. PLUGINA, unpublished). Besides, the strand displacement related mechanism is more suitable for recombination stimulated by various DNA damages (EPSTEIN 1958; CAMPBELL 1971; FRY 1979; SCHNEIDER, BERNSTEIN and BERNSTEIN 1978) and by ligase deficiency (EBISUZAKI and CAMPBELL 1969; KRISCH, SHAH and BERGER 1971). One

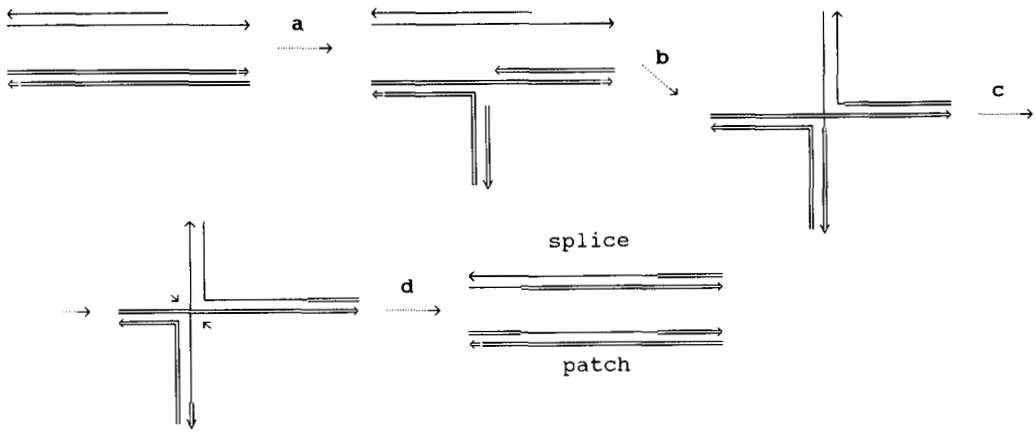


FIGURE 7.—SPC model variant with initiation of recombination via insertion of single-stranded 3′-terminus into a replication fork. After partial replication of one of the chromosomes (**a**) a single-stranded terminus of the other chromosome becomes inserted into the single-stranded gap near the replication fork (**b**). After some repair processing (removal of surplus termini, filling of gaps etc.), a Holliday structure emerges which, after branch migration (**c**) and breakage of the crossed strands (**d**), may give splice- and patch-containing linear DNA molecules.

may think that there exists more than one way to initiate recombination leading to the same final products. For example, chromosomal tips may play a major role early in the latent period, strand displacement being prevalent at later stages.

Quantitatively, the observed splice/patch coupling seems to be close to the maximum expected for the SPC model. We found that 29% of all the cells generating the recombinant *FC21-FC47* in cross I (the patch) produced also the recombinant *opX504* (the splice), with the maximum expected value being 50% (the other 50% of the patches being coupled with the reciprocal splice giving recombinant *amH72-FC21-FC47*). We already discussed above the inevitable underestimation of the coupled recombinant products in single bursts, so one should consider the pathway leading to coupled formation of splice and patch as the major one in the normal life cycle of T4 phage.

We do not think that the observed correlation between double and single exchanges was caused by reiterative recombinogenic action of chromosomal tips or by some other cell-to-cell as well as chromosome-to-chromosome recombination nonrandomness. Quite the opposite, we think that there are no serious arguments against formation of patches as primary recombination products (BERGER 1965; WIEMANN 1965), the patches and, to some extent, mismatch repair being able to explain all or nearly all high negative interference (TOOMPUU and SHCHERBAKOV 1980; SHCHERBAKOV *et al.* 1982b). The specificity of the observed correlation (between single and double exchanges) argues itself against its origin from more than random reiteration of recombinational events. It is evident that the reiteration would provide the same level of correlation between different single exchanges (cross III) as well as between different double exchanges (cross II) too. But in fact, the latter correlations were very low and they might be largely accounted for by the random coincidence of two different events in the same cell, as discussed above. Recombinational nonrandomness of any sort can account for little, if any, of the correlations observed here.

The surplus of mixed (*rII*$^+$ + *opal*) recombinant yields in cross II constituted 6% of all the *rII*$^+$ containing yields. Some surplus of mixed recombinant yields was observed also in the three-parental cross III. The corresponding value of coupling might be underestimated in this case because of the absence of the third mating partner in a certain proportion of the infected cells (at a multiplicity of infection one particle per cell the Poisson distribution predicts 37% of the cells were uninfected). After corresponding correction, we calculated a proportion of the mixed yields equal to 0.05 ± 0.02, *i.e.*, practically the same as for patch/patch coupling in cross II. Combined, these data give the proportion of mixed yields as 0.055 ± 0.006, the value differing significantly from zero but close to the values expected for in-the-same-cell coincidence.

Recalling earlier works on reciprocality of recombination in T2 phage by HERSHEY and ROTMAN (1949), we would like to make it clear that they had another goal and used a somewhat different approach. They studied correlations between recombinants of reciprocal genotypes. For example, in the two-factor cross *aB* × *Ab*, the recombinants *AB* and *ab* were determined in single bursts. Distances in the crosses were relatively large; hence, recombinants were produced mainly by splices. Speaking in terms of modern models, they studied the correlation between reciprocal splices, which are not expected to correlate according to the SPC model. The recombinant frequencies in the crosses analyzed were rather high, so that multiple recombination events had occurred in single cells, the quantitative correlation between the titers of reciprocal recombinants having been used as

a criterion for reciprocality of genetic exchanges. (In fact, they saw little correlation and concluded recombination was generally nonreciprocal.)

Because of the very low recombinant frequencies in our crosses (in the range of $10^{-5}$ to $10^{-4}$), we greatly reduced the possibility of independent formation of different recombinants in the same cell, so that most of the mixed yields were considered as cases of cosegregation. The observed values of coupling, *e.g.*, 0.29, thus have a physical sense quite different from that of the correlations estimated by HERSHEY and ROTMAN: our values (when doubled) are simply equal to the proportion of the splice/patch coupling pathway in general T4 recombination. As we discussed above, this proportion, once corrected for packaging losses, may be high enough to account for nearly all general recombination in T4 phage. We have, however, several lines of evidence for the operation of another, minor, pathway in T4 recombination, which results in the formation of only short (below 20 bp) patches (V. P. SHCHERBAKOV, L. A. PLUGINA and E. A. KUDRYASHOVA, in preparation), such as that presented in Figure 1 as event sequence **a** → **b**.

We are very grateful to BRITTA SWEBILIUS SINGER for generously supplying us with the T4 *rII* strains, and to ELIZABETH M. KUTTER for valuable discussion and help with manuscript preparation. We are indebted to TANYA KOLYSHEVA, LENA PARVITZKAYA and IRA SERGEYEVA for technical assistance.

## LITERATURE CITED

BEDINGER, P., and B. M. ALBERTS, 1983 The 3′-5′ proofreading exonuclease of bacteriophage T4 DNA polymerase is stimulated by other T4 DNA replication proteins. J. Biol. Chem. **258:** 9649–9656.

BERGER, H., 1965 Genetic analysis of T4D phage heterozygotes produced in the presence of 5-fluorodeoxyuridine. Genetics **52:** 729–746.

BROKER, T. R., 1973 An electron microscopic analysis of pathways for bacteriophage T4 DNA recombination. J. Mol. Biol. **81:** 1–16.

BROKER, T. R., and A. H. DOERMANN, 1975 Molecular and genetic recombination of bacteriophage T4. Annu. Rev. Genet. **9:** 213–244.

CAMPBELL, D. A., 1971 Analysis of multiplicity reactivation in X-irradiated bacteriophage T4D. Virology **44:** 188–199.

CURTIS, M. J., and B. ALBERTS, 1976 Studies on the structure of intracellular bacteriophage T4 DNA. J. Mol. Biol. **102:** 793–816.

DANNENBERG, R., and G. MOSIG, 1983 Early intermediates in bacteriophage T4 DNA replication and recombination. J. Virol. **45:** 813–831.

DOERMANN, A. H., 1973 T4 and the rolling circle model of replication. Annu. Rev. Genet. **7:** 325–341.

DOERMANN, A. H., and L. BOEHNER, 1963 An experimental analysis of bacteriophage T4 heterozygotes. I. Mottled plaques from crosses involving six *rII* loci. Virology **21:** 551–567.

DOERMANN, A. H., and D. H. PARMA, 1967 Recombination in bacteriophage T4. J. Cell. Physiol. **70** (suppl. I)**:** 147–164.

EBISUZAKI, K., and L. CAMPBELL, 1969 On the role of ligase in genetic recombination in bacteriophage T4. Virology **38:** 701–703.

EDGAR, R. S., 1961 High negative interference and heterozygosis: a study of the mechanism of recombination in bacteriophage T4. Virology **13:** 1–12.

ELLIS, E. L., and M. DELBRUCK, 1939 The growth of bacteriophage. J. Gen. Physiol. **22:** 365–384.

ENGLUND, P. T., 1971 The initial step of *in vitro* synthesis of deoxyribonucleic acid by the T4 deoxyribonucleic acid polymerase. J. Biol. Chem. **246:** 5684–5687.

EPSTEIN, R. H., 1958 A study of multiplicity reactivation in bacteriophage T4. I. Genetic and functional analysis of T4D-*K12*(λ) complexes. Virology **6:** 382–404.

EPSTEIN, R. H., A. BOLLE, C. M. STEINBERG, E. KELLENBERGER, B. E. DE LA TOUR, R. CHEVALLEY, R. S. EDGAR, M. SUSMAN, G. H. DENHARDT and I. LIELAUSIS, 1963 Physiological studies of conditional lethal mutants of bacteriophage T4D. Cold Spring Harbor Symp. Quant. Biol. **28:** 375–394.

FORMOSA, T., and B. M. ALBERTS, 1986a Purification and characterization of the T4 bacteriophage uvsX protein. J. Biol. Chem. **261:** 6107–6118.

FORMOSA, T., and B. M. ALBERTS, 1986b DNA synthesis dependent on genetic recombination: characterization of a reaction catalyzed by purified T4 proteins. Cell **47:** 793–806.

FRY, S. E., 1979 *Stimulation of recombination in phage T4 by* nitrous acid-induced lesions. J. Gen. Virol. **43:** 719–722.

GAREN, A., 1961 Physiological effects of *rII* mutations in bacteriophage T4. Virology **14:** 151–163.

GRIFFITH, J., and T. FORMOSA, 1985 *The uvsX protein of* bacteriophage T4 arranges single-stranded and double-stranded DNA into similar helical nucleoprotein filaments. J. Biol. Chem. **260:** 4484–4491.

HAMILTON, and D. E. PETTIJOHN, 1976 Properties of condensed bacteriophage T4 DNA isolated from *Escherichia coli* infected with bacteriophage T4. J. Virol. **19:** 1012–1027.

HAMLETT, N. V., and H. BERGER, 1975 Mutations altering genetic recombination and repair of DNA in bacteriophage T4. Virology **63:** 539–567.

HARRIS, L. D., and J. GRIFFITH, 1987 Visualization of the homologous pairing of DNA catalyzed by the bacteriophage T4 uvsX protein. J. Biol. Chem. **262:** 9285–9292.

HERSHEY, A. D., and R. ROTMAN, 1949 Genetic recombination between host range and plaque-type mutants of bacteriophage in single bacterial cells. Genetics **34:** 44–71.

HINTON, D. M., and N. G. NOSSAL, 1986 Cloning of bacteriophage T4 uvsX gene and purification and characterization of the T4 uvsX recombination protein. J. Biol. Chem. **261:** 5663–5673.

HOLLIDAY, R., 1964 A mechanism for gene conversion in fungi. Genet. Res. **5:** 282–304.

JENSCH, F., and B. KEMPER, 1986 Endonuclease VII resolves Y-junctions in branched DNA *in vitro*. EMBO J. **5:** 181–189.

HURST, D. D., S. FOGEL and R. K. MORTIMER, 1972 Conversion associated recombination in yeast. Proc. Natl. Acad. Sci. USA **69:** 101–105.

KEMPER, B., and E. JANZ, 1976 Function of gene 49 of bacteriophage T4. I. Isolation and biochemical characterization of very fast-sedimenting DNA. J. Virol. **18:** 992–999.

KEMPER, B., F. JENSCH, F. H.-J. DEPKA-PRONDZYNSKI, U. BORGMEYER and K. MIZUUCHI, 1984 Resolution of Holliday structures by endonuclease VII as observed in interactions with cruciform DNA. Cold Spring Harbor Symp. Quant. Biol. **49:** 815–825.

KODADEK, T., and M. L. WONG, 1990 Homologous pairing *in vitro* initiated by DNA synthesis. Biochem. Biophys. Res. Commun. **169:** 302–309.

KOZINSKI, A. W., and D. KOSTURKO, 1976 Late events in T4 bacteriophage production. II. Giant bacteriophages contain concatemers generated by recombination. J. Virol. **17:** 801–804.

KRISCH, H. M., D. B. SHAH and H. BERGER, 1971 Replication and recombination in ligase-deficient *rII* bacteriophage T4D. J. Virol. **7:** 491–498.

LUDER, A., and G. MOSIG, 1982 Two alternative mechanisms for initiation of DNA replication forks in bacteriophage T4: priming by RNA polymerase and by recombination. Proc. Natl. Acad. Sci. USA **79:** 1101–1105.

MESELSON, M. S., and C. M. RADDING, 1975 A general model for genetic recombination. Proc. Natl. Acad. Sci. USA **72:** 358–361.

MINOGAWA, T., A. MURAKAMI, Y. RYO and H. YAMAGISHI, 1983 Structural features of very fast sedimenting DNA formed by gene 49 defective T4. Virology **126:** 183–193.

MIZUUCHI, K., B. KEMPER, J. HAYS and R. A. WEISBERG, 1982 T4 endonuclease VII cleaves Holliday structures. Cell **29:** 357–365.

MOSIG, G., 1963 Genetic recombination in bacteriophage T4 during replication of DNA fragments. Cold Spring Harbor Symp. Quant. Biol. **28:** 35–42.

MOSIG, G., 1970 Recombination in bacteriophage T4. Adv. Genet. **15:** 1–53.

MOSIG, G., 1983 Relationship of T4 DNA replication and recombination, pp. 120–130 in *Bacteriophage T4*, edited by C. K. MATHEWS, E. M. KUTTER, G. MOSIG and P. B. BERGET. American Society for Microbiology, Washington, D.C.

MOSIG, G., D. GHOSAL and S. BOCK, 1981 Interactions between the maturation protein gp17 and the single-stranded DNA binding protein gp32 initiate DNA packaging and compete with initiation of secondary DNA replication forks in phage T4, pp. 139–150 in *Bacteriophage Assembly*, edited by M. DUBOW. Alan R. Liss, New York.

MOSIG, G., M. SHAW and G. M. GARCIA, 1984 On the role of DNA replication, endonuclease VII, and *rII* proteins in processing of recombinational intermediates in phage T4. Cold Spring Harbor Symp. Quant. Biol. **59:** 371–382.

MOSIG, G., R. EHRING, W. SCHLIEWEN and S. BOCK, 1971 The patterns of recombination and segregation in terminal regions of T4 DNA molecules. Mol. Gen. Genet. **113:** 51–91.

MOSIG, G., A. LUDER, G. GARCIA, R. DANNENBERG and S. BOCK, 1979 *In vivo* interactions of genes and proteins in DNA replication and recombination of phage T4. Cold Spring Harbor Symp. Quant. Biol. **43:** 501–515.

MOSIG, G., A. LUDER, L. ROWEN, P. MACDONALD and S. BOCK, 1981 On the role of recombination topoisomerase in primary and secondary initiation of T4 DNA replication, pp 277–295 in *The Initiation of Replication*, edited by D. RAY. Academic Press, New York.

MUELLER, J. E., B. KEMPER, R. P. CUNNINGHAM, N. R. KALLENBACH and N. C. SEEMAN, 1988 T4 endonuclease VII cleaves the crossover strands of Holliday junction analogs. Proc. Natl. Acad. Sci. USA **85:** 9441–9445.

MUZYCZKA, N., R. L. POLAND and M. J. BESSMAN, 1972 Studies on the biochemical basis of spontaneous mutation. I. A comparison of the deoxyribonucleic acid polymerases of mutator, antimutator and wild type strains of bacteriophage T4. J. Biol. Chem. **247:** 7116–7122.

PRIBNOW, D., D. C. SIGURDSON, L. GOLD, B. S. SINGER, C. NAPOLI, J. BROSIUS, T. J. DULL and H. F. NOLLER, 1981 *rII* cistrons of bacteriophage T4. DNA sequence around intercistronic divide and positions of genetic landmarks. J. Mol. Biol. **149:** 337–376.

SCHNEIDER, S., C. BERNSTEIN and H. BERNSTEIN, 1978 Recombinational repair of alkylation lesions in phage T4. I. *N*-Methyl-*N'*-nitro-*N*-nitrosoguanidine. Mol. Gen. Genet. **167:** 185–195.

SHAH, D. B., and H. BERGER, 1971 Replication of gene 46–47 *amber* mutants of bacteriophage T4D. J. Mol. Biol. **57:** 17–34.

SHAH, D. B., and L. DELORENZO, 1977 Suppression of gene 49 mutations of bacteriophage T4 by a second mutation in gene *x*: structure of pseudorevertant DNA. J. Virol. **24:** 794–804.

SHCHERBAKOV, V. P., and L. PLUGINA, 1991 Marker-dependent recombination in T4 bacteriophage. III. Structural prerequisites for marker discrimination. Genetics **128:** 673–685.

SHCHERBAKOV, V. P., L. A. PLUGINA, E. A. KUDRYASHOVA, O. I. EFREMOVA, S. T. SIZOVA and O. G. TOOMPUU, 1982a Marker-dependent recombination in T4 bacteriophage. I. Outline of the phenomenon and evidence suggesting a mismatch repair mechanism. Genetics **102:** 615–625.

SHCHERBAKOV, V. P., L. A. PLUGINA, E. A. KUDRYASHOVA, O. I. EFREMOVA, S. T. SIZOVA and O. G. TOOMPUU, 1982b Marker-dependent recombination in T4 bacteriophage. II. The evaluation of mismatch repairabilities in crosses within indicator distances. Genetics **102:** 627–637.

SHIBATA, T., C. DASGUPTA, R. P. CUNNINGHAM and R. C. RADDING, 1980 Homologous pairing in genetic recombination: Formation of D loops by combined action of recA protein and a helix-destabilizing protein. Proc. Natl. Acad. Sci. USA **77:** 2606–2610.

SIGAL, N., and B. ALBERTS, 1972 Genetic recombination: The nature of a crossed-strand exchange between two homologous DNA molecules. J. Mol. Biol. **71:** 789–793.

STAHL, F. W., 1979 *Genetic Recombination. Thinking about It in Phage and Fungi*. W. H. Freeman, San Francisco.

TOOMPUU, O. G., and V. P. SHCHERBAKOV, 1980 Genetic recombination: formal implications of a crossed-strand exchange between two homologous DNA molecules. J. Theor. Biol. **82:** 497–520.

UHLENHOPP, F. L., B. H. ZIMM and D. J . CUMMINGS, 1974 Structural aberrations in T-even bacteriophage. VI. Molecular weight of DNA from giant heads. J. Mol. Biol. **89:** 689–702.

WATSON, J. D., 1972 Origin of concatemeric T7 DNA. Nature New Biol. **239:** 197–201.

WIEMANN, J., 1965 Zur Charaktersierung von Heterozygoten des Phagen T4. Z. Vererbungsl. **97:** 81–101.

WOMACK, F. C., 1963 An analysis of single-burst progeny of bacteria singly infected with a bacteriophage heterozygote. Virology **21:** 232–241.

YONESAKI, T., and T. MINOGAWA, 1985 T4 phage gene *uvsX* product catalyzes homologous DNA pairing. EMBO J. **4:** 3321–3327.

YONESAKI, T., and T. MINOGAWA, 1989 Synergistic action of three recombination gene products of bacteriophage T4, *uvsX*, *uvsY*, and gene 32 proteins. J. Biol. Chem. **264:** 7814–7820.

YONESAKI, T., Y. RYO, T. MINOGAWA and H. TAKAHASHI, 1985 Purification and some of the functions of the products of the bacteriophage T4 recombination genes uvsX and uvsY. Eur. J. Biochem. **148:** 127–134.

Communicating editor: G. R. SMITH